IOP Conf. Series: Materials Science and Engineering **103** (2015) 012021 doi:10.1088/1757-899X/103/1/012021

Effect of ageing on phase evolution and precipitation behaviour of duplex steel

P Podany[1], M Kover and J Dlouhy

COMTES FHT a.s., Prumyslova 995, 334 41 Dobrany, Czech Republic

E-mail: pavel.podany@comtesfht.cz

Abstract. The isothermal formation of secondary phases in duplex stainless steel was studied. Samples were isothermally heat treated (aged) at temperatures of 700, 800 and 850°C in a quenching dilatometer. Microstructured evolution of secondary phases was analysed by means of optical and scanning electron microscopes. Both common phases, Chi and Sigma, were observed. The resulting shrinkage curves from dilatometric measurements show the potential for research into the formation of minor phases and the estimation of transformation kinetics in this kind of steel.

1. Introduction

The duplex family of stainless steels (DSS) is composed of a mixture of ferrite and austenite and combines some typical properties of each of these phases. The duplex microstructure and chemical composition lead to high strength and good resistance to corrosion, abrasion and wear [1]. Different grades of DSS are increasingly used to store and transport highly corrosive fluids and gases in a wide range of industry sectors. A further enhancement to the mechanical properties and corrosion resistance of DSS can be achieved by the addition of various alloying elements, such as chromium, nickel, molybdenum, tungsten, nitrogen etc [2].

However, this alloying could also lead to microstructure or phase instability and thus to matrix depletion of the main alloying elements (e.g., chromium, molybdenum, and niobium) connected with the formation of secondary phases at high temperatures associated with processing forging, heat treatment or during the service itself. Several precipitation reactions usually occur when this steel is exposed in the specific temperature range. Usually it is between 600 and 1300°C. It especially leads to the precipitation of secondary phases: χ - Chi, σ - Sigma, carbides and nitrides [2]. Of all these phases, the Sigma phase is the most important, as its formation is accompanied by a decrease in ductility and toughness, especially if these are measured at normal temperatures. It is an intermetallic compound with a tetragonal crystal structure. In the mixture with the alpha phase, the Sigma phase contains between 20 and 70 wt. % chromium at relatively long thermal exposure times in the interval between 500 and 900°C. It is possible to put the resulting Fe-Cr Sigma phase into solid solution using short-time heating (for 1 hour or more). Fe-Cr alloys with manganese, nickel and molybdenum require longer times or higher temperatures for the Sigma phase to dissolve [3].

In recent years, great effort has been devoted to research into the precipitation of the Sigma phase and Chi phase in duplex steels. In general, the Sigma phase is considered undesirable as it depletes the

[1] Address for correspondence: P Podany, COMTES FHT a.s., Prumyslova 995, 334 41 Dobrany, Czech Republic. E-mail: pavel.podany@comtesfht.cz.

matrix of chromium. This depletion impairs the material's resistance to pitting corrosion. On the other hand, presence of the Sigma phase increases the creep resistance of the material [4].

The research into precipitation of the above phases focused on how some alloying elements suppress this precipitation during annealing. For instance, Kang, et al. showed that substituting part of the molybdenum content with tungsten suppresses precipitation of the Sigma phase. Like molybdenum, tungsten is known to improve resistance to pitting corrosion [5, 6]. Akisanya, et al. studied super duplex steels with increased tungsten content. They explored the effect of age hardening on mechanical properties [2]. Other studies indicate that adding a small amount of cerium helps to suppress the precipitation of secondary phases. Kim S, et al. has proven that adding 50-100 ppm cerium inhibits precipitation of the Sigma and Chi phases. If the cerium content is increased to 450 ppm, it merely leads to the formation of cerium-rich particles and the depletion of cerium in the matrix. In such case, cerium cannot suppress the precipitation [7]. Similarly, Yoo Y H, et al. studied the effects of alloying with cerium and other rare earth elements, lanthanum and barium [8]. According to Jeon S H, et al., another element that suppresses precipitation of the Sigma phase is copper. According to their results, adding approx. 1.30% copper practically eliminates precipitation of the Sigma phase and causes a slight increase in precipitation of the Chi phase. Despite that, the resulting total amount of secondary phases is smaller than without the addition of copper [9, 10]. As the above studies show, the precipitation of undesirable phases can be effectively controlled by adding some elements to the material. Despite that, designers are frequently required to use a particular commercially available grade of material specified by clients. It is, therefore, important to know the temperature ranges and heat treating sequences which lead to the precipitation of unwanted phases that can substantially alter the corrosion resistance, as well as the mechanical properties of the material. In the presented paper, the authors used a quenching dilatometer to study the precipitation process and to carry out the heat treatment. The purpose was to map primarily the initial stages of Sigma phase precipitation within three ranges of age hardening temperatures for a particular heat.

2. Experimental methods

2.1. Experimental material and sampling

The chemical composition of the experimental material is shown in table 1. The material was supplied in the form of forged pieces of 120 × 120 mm cross-section. Specimens were taken from the forged pieces for dilatometric measurement. The diameter and length of these specimens were 4 mm and 10 mm, respectively. After dilatometric measurement, these specimens were used for making longitudinal metallographic sections. As the other authors of research institute showed earlier [11], these specimens can also be used for making miniature mechanical testing specimens.

Table 1. Chemical composition (wt %) of experimental steel.

C	Si	Mn	P	S	Cu	Cr	Ni	Mo	Ti	W	N	Fe
0.032	0.316	1.449	0.017	0.007	0.084	21.771	5.660	3.138	0.002	0.023	0.135	bal

2.2. Dilatometric experiments

Samples with a length of 10 mm and a diameter of 4 mm were heat treated in the quenching dilatometer Linseis L78 RITA. The temperature was measured and controlled by a type K thermocouple, welded to the sample centre. The length change was measured by an LVDT sensor through a quartz push-rod. The dilatometric measurements were performed in a protective environment (He). Heating was performed using an inductive coil. The sample was cooled with protective gas. Prior to heat treatment, the sample chamber was refilled (evacuated and filled with He gas) three times. The samples were solution annealed at 1100°C for 1 hour, quenched at the rate of 180°C/s and aged at 700°C, 800°C and 850°C.

2.3. Characterisation of microstructure and phases

The microstructure was studied on the metallographic sections through the dilatometer specimens. The microstructure was revealed using two-phase electrolytic etching. The first stage involved a voltage of 5.5 V applied for 20s in combination with 10% oxalic acid. In the second stage, a voltage of 2.3 V was used for 8 s with 20% NaOH. In the first stage, the precipitates are attacked. In the second stage, the ferrite becomes coloured. The microstructure was documented using a Zeiss Axio Observer optical microscope. Specimens for scanning electron microscopy were etched with Beraha's reagent. Quantitative image analysis was carried out using NIS-Elements software. EBSD analysis was performed and scanning electron micrographs taken by means of JEOL 6380 and JEOL 7400F microscopes and an HKL Nordlys EBSD (Electron backscatter diffraction) camera from Oxford Instruments.

3. Results and discussion

3.1. Evolution of microstructure during aging

The as-received microstructure of the forged stock is shown in Fig. 1. In the micrograph, ferrite appears dark, whereas austenite appears bright. The quantitative analysis of phases by means of the NIS Elements software showed a ferrite fraction of 49.6%. No intermediate phases were found in the as-received microstructure. The same applies to the microstructure of solution-annealed specimens (Figs. 1(a) and 1(b)).

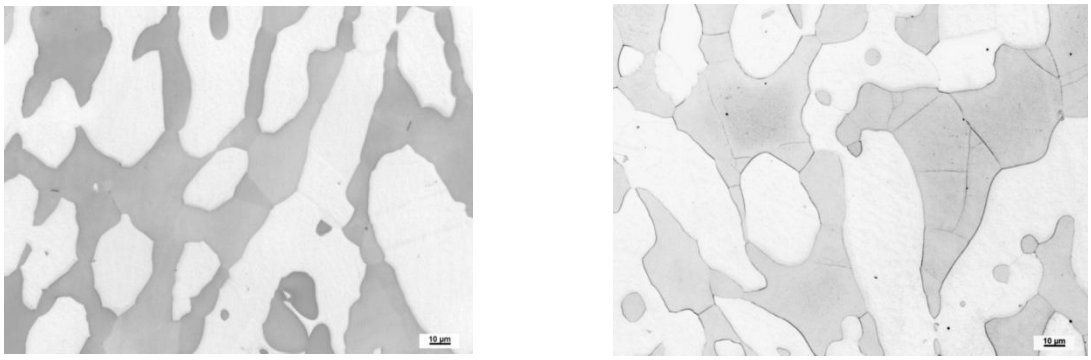

(a) As-received state (forged)-2-phase electrolytic etching

(b) After solution annealing-2-phase electrolytic etching

Figure 1. Microstructure of analysed duplex steel.

The microstructure evolution with the increasing holding time at 800°C is illustrated in Figs. 2(a)-2(d). As these figures show, the amount of the Chi and Sigma phase increases with increasing annealing time (see Figs. 2(a)-2(c)) up to 16,000s. When the Sigma phase is developed, the Chi phase starts to transforms into the Sigma phase and the amount of the Chi phase decreases (compare Figs. 2(c) and 2(d)). This assumption has been confirmed by other studies, as well [12].

Several basic shapes of intermediate phase particles were found in the microstructures. The Chi phase occurs first on grain boundaries at the ferrite-austenite interface. Later, it can be found on grain boundaries within the ferrite. Its particles are of irregular shape and sometimes elongated. They appear light grey in backscattered electron micrographs. This is due to the higher level of molybdenum than in the Sigma phase. The Sigma phase appears dark grey (2). According to other authors, chromium carbonitrides often precipitate together with the Chi phase [13-14]. This seems to be confirmed by figure 3. It shows very small precipitates on grain boundaries in a specimen annealed at 850°C for 107 seconds. Due to their size, their chemical composition could not be measured using EDX.

The Sigma phase occurs both in the interior of the original ferrite grains and as precipitates within the Chi phase particles which are found on the grain boundaries [12]. For the purpose of monitoring the precipitation of various phases and carbonitrides in steel, the use of electrolytic etching with oxalic acid has proven very useful. It is clear that even those particles which are too small to be resolved by

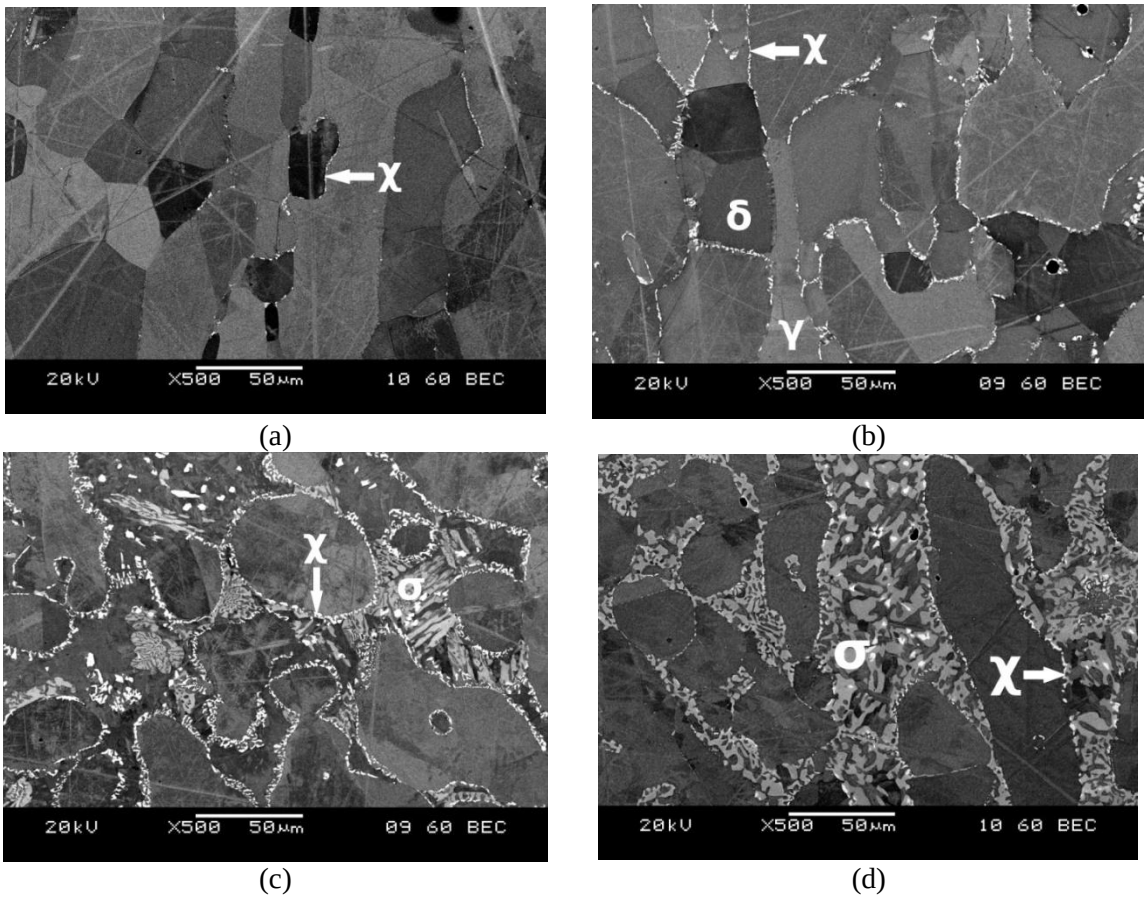

Figure 2. The microstructure of the experimental steel after ageing at 800℃ for (a) 1000s, (b) 3,600s, (c) 16,000s, and (d) 230,000s.

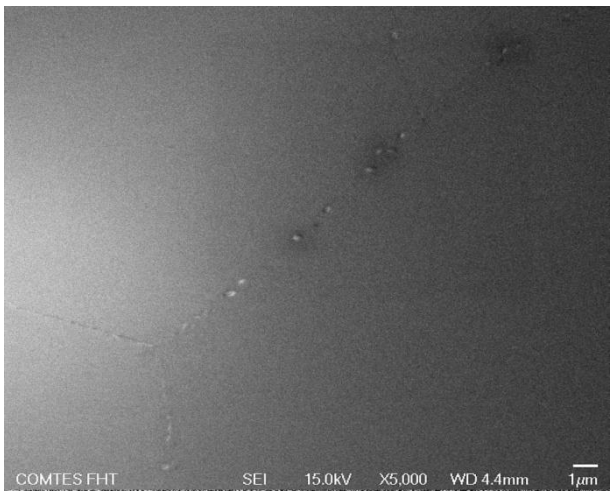

Figure 3. Sample aged at 850℃ for 107s – precipitation of Chi or CrC(N).

scanning electron microscopy can initiate a very vigorous reaction between the etchant and the specimen surface, leading to an intensive attack on the particle and its immediate vicinity. For illustration, optical micrographs of specimens etched with oxalic acid and backscattered scanning electron micrographs of identical polished specimens are shown in Figs. 4(a) and 4(b). Using specimens etched with oxalic acid to document microstructure by means of scanning electron

microscopy is not useful, as the Chi phase, carbonitrides and other phases are completely etched away by the electrolyte.

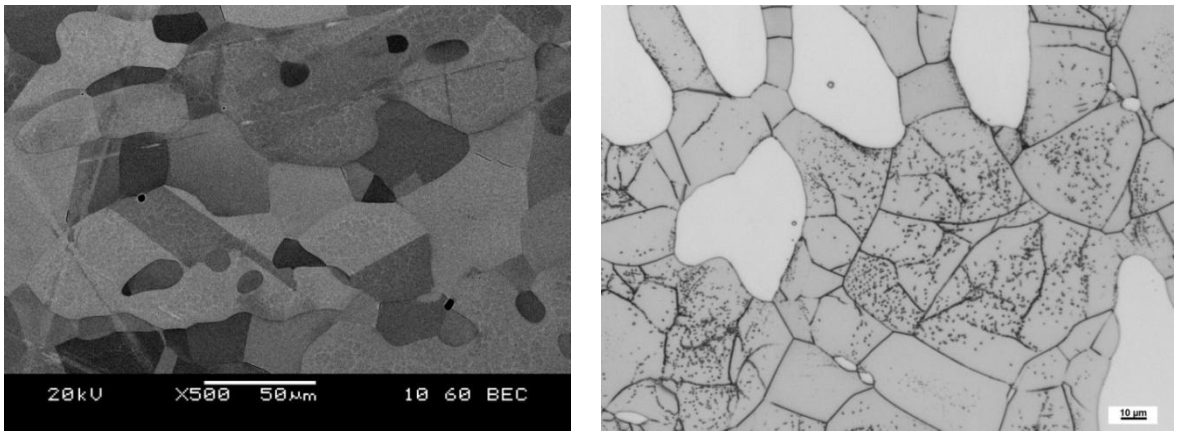

(a) BSE signal on SEM (b) Two-phase electrolytic etching

Figure 4. Microstructure of sample aged at 700℃ for 156s.

3.2. EBSD analyses

Fig. 5 shows an EBSD (Electron backscatter diffraction) micrograph of the steel sample aged at 800°C for 16,000 s. The Sigma phase (coloured yellow in Fig. 5(b)) was clearly detected. The Chi phase is difficult to distinguish (by EBSD) between the ferrite and austenite because it has a cubic lattice [14].

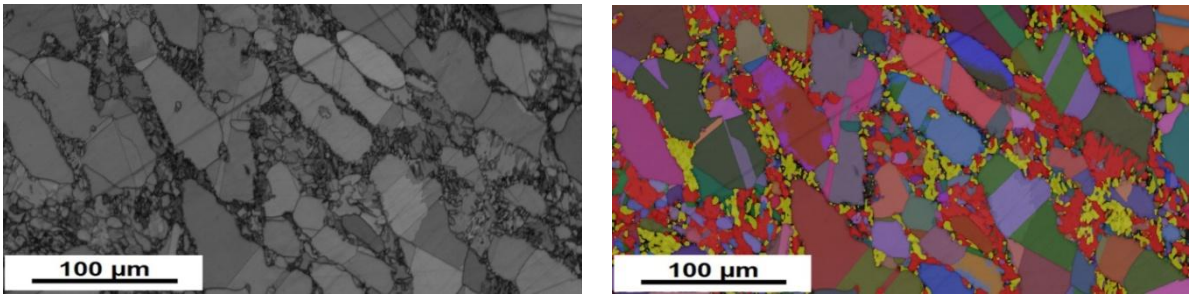

(a) Band contrast (b) EBSD mapping (Sigma - yellow, ferrite – red, austenite – orientfigation)

Figure 5. EBSD microstructure of sample aged at 800℃ for 16,000s.

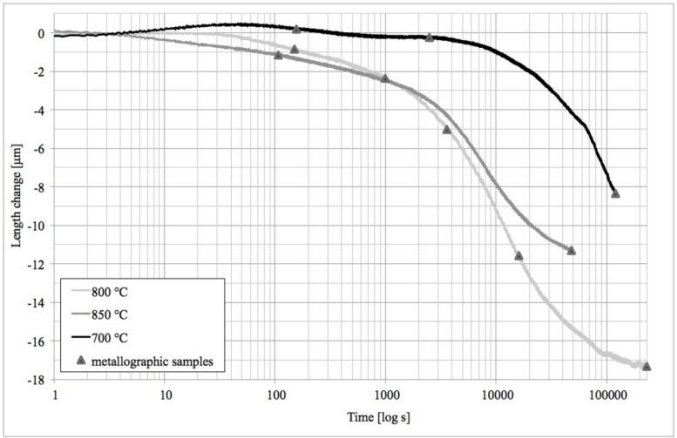

Figure 6. Shrinkage of the samples during ageing.

3.3. Dilatometric curves

During isothermal ageing in the dilatometer, shrinkage of all samples was observed. However, the length change at 700°C differs from the length change at 800°C and 850°C (figure 6). This behaviour might be attributed to different equilibrium phase ratios and ageing kinetics. Similar conclusions were stated in [13-16]. The initial length increase at 700°C might be attributed to the transport of the alloying elements to future nucleation sites. According to SEM observation, the first rapid decrease in length is a result of the formation of austenite, carbides and nitrides. Nucleation of the Chi and Sigma phases is expected to follow, leading to less shrinkage because the contraction during the phase formation at the interface is compensated by transport of the alloying elements. As the Sigma phase grows into ferrite grains, the shrinkage decreases even more. Formation of the Chi and Sigma phases cannot be distinguished from each other, although their formation kinetics is obvious from the curves. The most visible differences between the kinetics relate to nitride and Sigma/Chi formation at 700°C. The nucleation phase was estimated for all temperatures. The final phase of the ageing process was estimated for 800°C and 850°C. The estimated Chi and Sigma phase formation start and end times are listed in table 2.

Table 2. Estimated start and end of Chi and Sigma formation.

Temperature [°C]	Chi/Sigma formation start [s]	Chi/Sigma formation end [s]
700	2500	-
800	151	120,000
850	107	48,000

4. Conclusion

According to the results presented here, a quenching dilatometer can be used not only for precise heat treatment, but also for research into the formation of minor phases and estimation of transformation kinetics in duplex steels. The formation of precipitates led to contraction. The length change, which reflects the transformation kinetics, has a typical “S shape” in the logarithmic time graph. Although the early stage of Chi and Sigma precipitation could not be determined by SEM, a future TEM investigation might confirm the nucleation start identified by means of a dilatometer.

Very early stages of precipitation of undesirable phases can be observed using optical microscopy and specimens following electrolytic etching with oxalic acid. For instance, the Chi phase becomes fully discernible using the backscattered electron mode in scanning electron microscopy only after the specimens have been isothermally held for an extensive period of time, although evidence from both electrolytically etched specimens and dilatometric curves shows that precipitation occurs earlier.

Acknowledgment

These results were created under the project entitled Development of West-Bohemian Centre of Materials and Metallurgy No.: LO1412, financed by the Ministry of Education, Youth and Sports of the Czech Republic.

References

[1] Nilsson J O, et al 1992 Super duplex stainless steel *Mater. Sci. Technol.* **8** 685-700
[2] Akisanya A R, Obi U and Renton N C 2012 Effect of ageing on phase evolution and mechanical properties of a high tungsten super-duplex stainless steel *Materials Science and Engineering A* **535** 281-9
[3] Chvatalova K 2007 First-principles calculations of the total energy of systems of ordered structures of transition metals (Faculty of Science, Masaryk University: Dissertation thesis)
[4] Shek C H, Li D J, Wong K W and Lai J K L 1999 Creep properties of aged duplex stainless steels containing σ phase *Materials Science and Engineering A* **266** 30-6
[5] Kang T H, Li D M, Lee Y D and Lee C S 1998 Alloying and aging effects on the fatigue crack growth of duplex stainless steels *Materials Science and Engineering A* **251** 192-9

[6] Jeon S H, Kim S T, Lee I S, Kim J S, Kim K T and Park Y S 2012 Effects of W substitution on the precipitation of secondary phases and the associated pitting corrosion in hyper duplex stainless steels *Journal of Alloys and Compounds* **544** 166-72
[7] Sun M K, Ji S K, Kim K T, Park K T and Chong S L 2013 Effect of Ce addition on secondary phase transformation and mechanical properties of 27Cr–7Ni hyper duplex stainless steels *Materials Science and Engineering A* **573** 27-36
[8] Yoo Y H, Choi Y S, Kim J G and Park Y S 2010 Effects of Ce, La and Ba addition on the electrochemical behavior of super duplex stainless steels *Corrosion Science* **52** 1123-9
[9] Jeon S H, Kim S T, Lee I S, Kim J S, Kim K T and Park Y S 2013 Effects of Cu on the precipitation of intermetallic compounds and the intergranular corrosion of hyper duplex stainless steels *Corrosion Science* **66** 217-24
[10] Ran Q, Xu Y, Li J, Wan J, Xiao X and Yu H 2013 Effect of heat treatment on transformation-induced plasticity of economical Cr19 duplex stainless steel *Materials and Design* **46** 758-65
[11] Dzugan J and Konopik P 2012 Small punch test application to material properties evolution determination *Journal of Solid Mechanics and Materials Engineering* **6** 782-91
[12] Calliari I, Pellizzari M and Ramous E 2011 Precipitation of secondary phases in super duplex stainless steel ZERON100 isothermally aged *Materials Science and Technology* **27** 928-32
[13] Fritz J D 2003 Effects of metallurgical variables on the corrosion of stainless steels in ASM *Handbook Volume 13A Corrosion: Fundamentals, Testing, and Protection* pp 266-74
[14] Kim Y J, Ugurlu O, Jiang C, Gleeson B and Chumbley L S 2007 Microstructural evolution of secondary phases in the cast duplex stainless steels CD3MN and CD3MWCuN *Metallurgical and Materials Transactions A* **38** 203-11
[15] Elmer J W, Palmer T A and Specht E D 2003 Direct observations of sigma phase formation in duplex stainless steels using In situ synchrotron X-ray diffraction *Metallurgical Transactions A* **38** 464-75
[16] Magnabosco R 2009 Kinetics of sigma phase formation in a duplex stainless steel *Mat. Res.* **12** 321-7